

# Aircraft Data for the Real-Time Flight Simulation

Copyright © 2019 Marek M. Cel. All rights reserved.

Author: Marek M. Cel

Revision: 4

Date: 2019-12-14

This work is licensed under a

**Creative Commons CC0 1.0 Universal Public Domain Dedication**

### **Statement of Purpose**

The laws of most jurisdictions throughout the world automatically confer exclusive Copyright and Related Rights (defined below) upon the creator and subsequent owner(s) (each and all, an "owner") of an original work of authorship and/or a database (each, a "Work").

Certain owners wish to permanently relinquish those rights to a Work for the purpose of contributing to a commons of creative, cultural and scientific works ("Commons") that the public can reliably and without fear of later claims of infringement build upon, modify, incorporate in other works, reuse and redistribute as freely as possible in any form whatsoever and for any purposes, including without limitation commercial purposes. These owners may contribute to the Commons to promote the ideal of a free culture and the further production of creative, cultural and scientific works, or to gain reputation or greater distribution for their Work in part through the use and efforts of others.

For these and/or other purposes and motivations, and without any expectation of additional consideration or compensation, the person associating CC0 with a Work (the "Affirmer"), to the extent that he or she is an owner of Copyright and Related Rights in the Work, voluntarily elects to apply CC0 to the Work and publicly distribute the Work under its terms, with knowledge of his or her Copyright and Related Rights in the Work and the meaning and intended legal effect of CC0 on those rights.

**1. Copyright and Related Rights.** A Work made available under CC0 may be protected by copyright and related or neighboring rights ("Copyright and Related Rights"). Copyright and Related Rights include, but are not limited to, the following:

- i. the right to reproduce, adapt, distribute, perform, display, communicate, and translate a Work;
- ii. moral rights retained by the original author(s) and/or performer(s);
- iii. publicity and privacy rights pertaining to a person's image or likeness depicted in a Work;
- iv. rights protecting against unfair competition in regards to a Work, subject to the limitations in paragraph 4(a), below;

- v. rights protecting the extraction, dissemination, use and reuse of data in a Work;
- vi. database rights (such as those arising under Directive 96/9/EC of the European Parliament and of the Council of 11 March 1996 on the legal protection of databases, and under any national implementation thereof, including any amended or successor version of such directive); and
- vii. other similar, equivalent or corresponding rights throughout the world based on applicable law or treaty, and any national implementations thereof.

**2. Waiver.** To the greatest extent permitted by, but not in contravention of, applicable law, Affirmer hereby overtly, fully, permanently, irrevocably and unconditionally waives, abandons, and surrenders all of Affirmer's Copyright and Related Rights and associated claims and causes of action, whether now known or unknown (including existing as well as future claims and causes of action), in the Work (i) in all territories worldwide, (ii) for the maximum duration provided by applicable law or treaty (including future time extensions), (iii) in any current or future medium and for any number of copies, and (iv) for any purpose whatsoever, including without limitation commercial, advertising or promotional purposes (the "Waiver"). Affirmer makes the Waiver for the benefit of each member of the public at large and to the detriment of Affirmer's heirs and successors, fully intending that such Waiver shall not be subject to revocation, rescission, cancellation, termination, or any other legal or equitable action to disrupt the quiet enjoyment of the Work by the public as contemplated by Affirmer's express Statement of Purpose.

**3. Public License Fallback.** Should any part of the Waiver for any reason be judged legally invalid or ineffective under applicable law, then the Waiver shall be preserved to the maximum extent permitted taking into account Affirmer's express Statement of Purpose. In addition, to the extent the Waiver is so judged Affirmer hereby grants to each affected person a royalty-free, non transferable, non sublicensable, non exclusive, irrevocable and unconditional license to exercise Affirmer's Copyright and Related Rights in the Work (i) in all territories worldwide, (ii) for the maximum duration provided by applicable law or treaty (including future time extensions), (iii) in any current or future medium and for any number of copies, and (iv) for any purpose whatsoever, including without limitation commercial, advertising or promotional purposes (the "License"). The License shall be deemed effective as of the date CC0 was applied by Affirmer to the Work. Should any part of the License for any reason be judged legally invalid or ineffective under applicable law, such partial invalidity or ineffectiveness shall not invalidate the remainder of the License, and in such case Affirmer hereby affirms that he or she will not (i) exercise any of his or her remaining Copyright and Related Rights in the Work or (ii) assert any associated claims and causes of action with respect to the Work, in either case contrary to Affirmer's express Statement of Purpose.

**4. Limitations and Disclaimers.**

- a. No trademark or patent rights held by Affirmer are waived, abandoned, surrendered, licensed or otherwise affected by this document.
- b. Affirmer offers the Work as-is and makes no representations or warranties of any kind concerning the Work, express, implied, statutory or otherwise, including without limitation warranties of title, merchantability, fitness for a particular purpose, non infringement, or the absence of latent or other defects, accuracy, or the present or absence of errors, whether or not discoverable, all to the greatest extent permissible under applicable law.
- c. Affirmer disclaims responsibility for clearing rights of other persons that may apply to the Work or any use thereof, including without limitation any person's Copyright and Related Rights in the Work. Further, Affirmer disclaims responsibility for obtaining any necessary consents, permissions or other rights required for any use of the Work.
- d. Affirmer understands and acknowledges that Creative Commons is not a party to this document and has no duty or obligation with respect to this CC0 or use of the Work.

## Table of Contents

Notation.....	6
1. Geometric Parameters.....	7
1.1. Wing Basic Geometric Parameters.....	7
1.2. Mean Aerodynamic Chord.....	7
1.3. Wing Aerodynamic Center.....	8
2. Aerodynamic Characteristics.....	9
2.1. Aerodynamic Characteristics Approximation.....	9
2.2. Finite Wing Aerodynamic Characteristics.....	11
2.3. Horizontal Tail Incidence.....	11
2.4. Critical Angle of Attack.....	12
3. Mass and Inertia Data.....	14
3.1. Structure Groups Breakdown.....	14
3.2. OpenVSP.....	14
4. Computational Fluid Dynamics.....	15
4.1. Tools.....	15
4.1.1. XFOIL.....	15
4.1.2. VSPAERO.....	15
4.1.3. OpenFOAM.....	15
4.2. Workflow.....	15
4.2.1. XFOIL.....	15
4.2.2. VSPAERO.....	16
4.2.3. OpenFOAM.....	18
4.3. Results.....	28
4.3.1. XFOIL.....	28
4.3.2. VSPAERO.....	30
4.3.3. OpenFOAM.....	31
Bibliography.....	33

## Notation

$a = \frac{dC_L}{d\alpha}$	– [1/rad] lift curve slope
$A = \frac{b^2}{S}$	– [-] wing aspect ratio
$b$	– [m] wing span
$c_{root}$	– [m] chord at wing root
$c_{tip}$	– [m] chord at wing tip
$c_{MAC}$	– [m] mean aerodynamic chord
$C_D$	– [-] drag coefficient
$C_l$	– [-] rolling moment coefficient
$C_L$	– [-] lift coefficient
$C_m$	– [-] pitching moment coefficient
$C_n$	– [-] yawing moment coefficient
$C_Y$	– [-] side force coefficient
$C_\mu$	– [-] k-ε turbulence model constant
$d$	– [m] fuselage diameter
$D$	– [N] drag
$e$	– [-] Oswald efficiency factor
$i$	– [rad] incidence angle
$I$	– [-] turbulence intensity
$k$	– [m <sup>2</sup> /s <sup>2</sup> ] turbulence kinetic energy
$L$	– [N] lift
$L$	– [m] reference length scale
$p$	– [Pa] pressure
$Re$	– [-] Reynolds number
$S$	– [m <sup>2</sup> ] wing area
$V$	– [m/s] velocity
$\alpha$	– [rad] angle of attack
$\beta$	– [rad] angle of sideslip
$\lambda = \frac{c_{tip}}{c_{root}}$	– [-] wing taper ratio
$\Lambda_{LE}$	– [rad] leading edge sweep angle
$\Lambda_{t/c}$	– [rad] sweep angle at maximum thickness
$\omega$	– [1/s] specific turbulence dissipation rate
$\frac{\partial \epsilon}{\partial \alpha}$	– [-] horizontal stabilizer downwash angle derivative with respect to the aircraft angle of attack

## 1. Geometric Parameters

### 1.1. Wing Basic Geometric Parameters

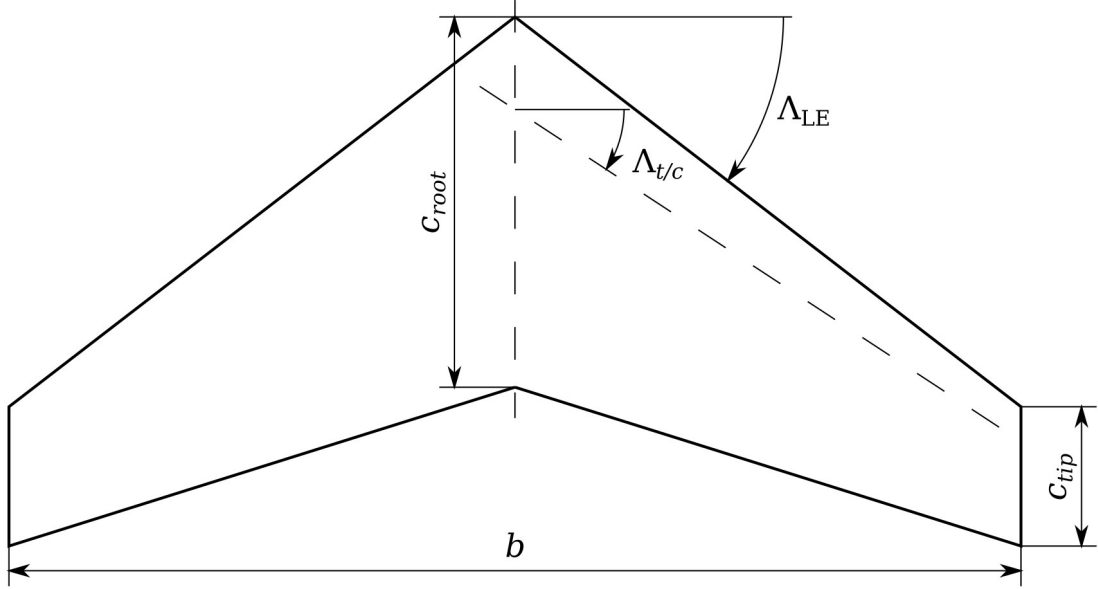


Figure 1-1: Wing basic geometric parameters

Aspect ratio is given by the following formula. [1]

$$A = \frac{b^2}{S} \quad (1.1)$$

Taper ratio is given by the following formula. [1]

$$\lambda = \frac{c_{tip}}{c_{root}} \quad (1.2)$$

### 1.2. Mean Aerodynamic Chord

For taper wing mean aerodynamic chord can be calculated using following formula. [2]

$$c_{MAC} = \frac{2}{3} c_{root} \frac{1 + \lambda + \lambda^2}{1 + \lambda} \quad (1.3)$$

For more complex shapes mean aerodynamic chord is given as follows. []

$$c_{MAC} = \left( \int_{-\frac{b}{2}}^{\frac{b}{2}} (c(y))^2 dy \right) \div \left( \int_{-\frac{b}{2}}^{\frac{b}{2}} c(y) dy \right) \quad (1.4)$$

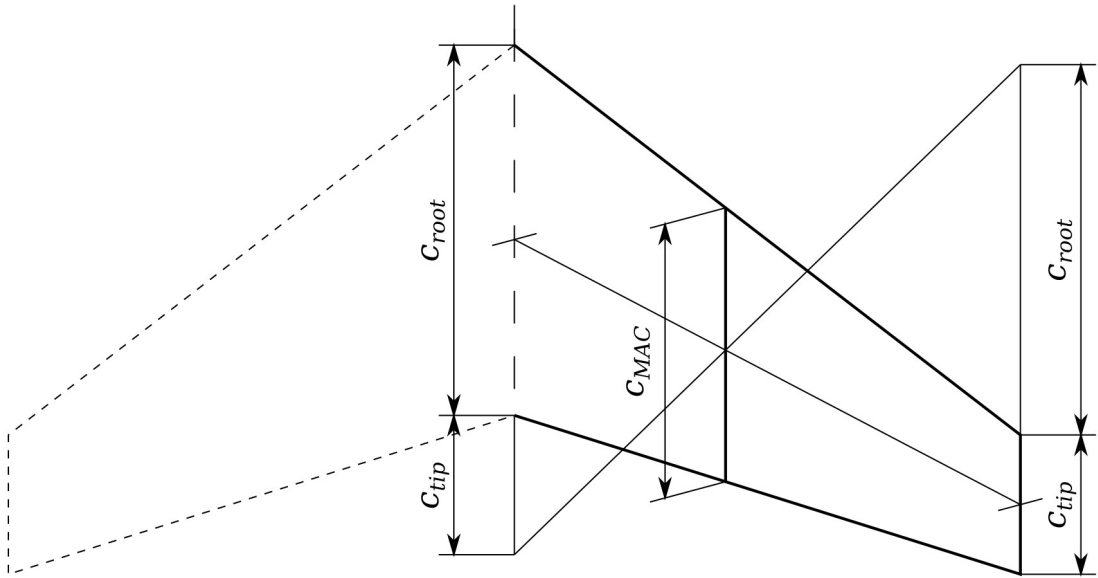


Figure 1-2: Mean aerodynamic chord

### 1.3. Wing Aerodynamic Center

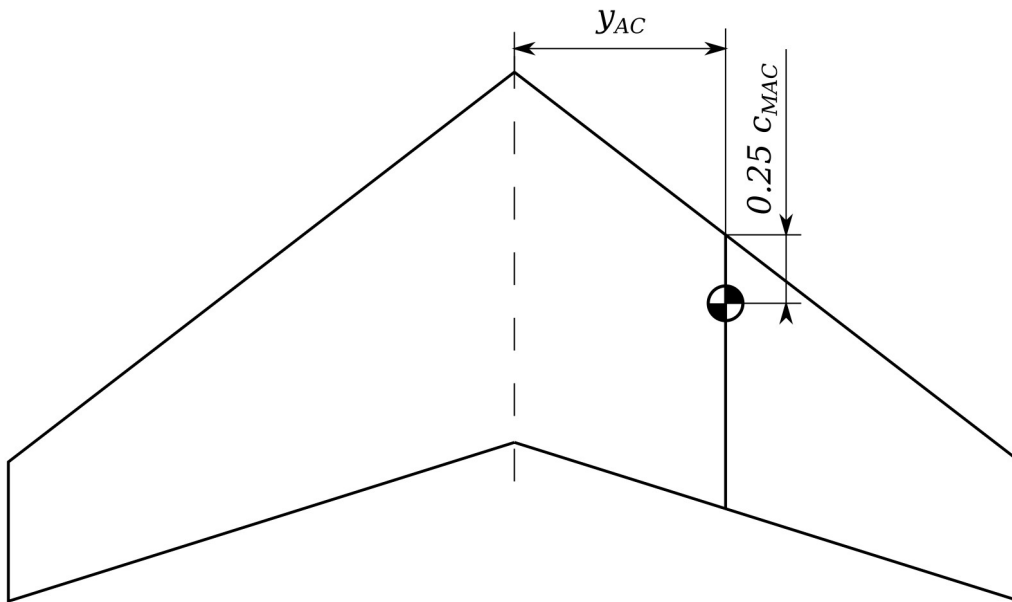


Figure 1-3: Wing aerodynamic center

Position of wing aerodynamic center  $\vec{r}_{AC}$  is at 25% of the mean aerodynamic chord and its lateral coordinate is given by the following formula. [1], [2], [3]

$$y_{AC} = \frac{b(1+2\lambda)}{6(1+\lambda)} \quad (1.5)$$



## 2. Aerodynamic Characteristics

### 2.1. Aerodynamic Characteristics Approximation

Following approximation is used to get lift coefficient for the full range of angle of attack. [4]

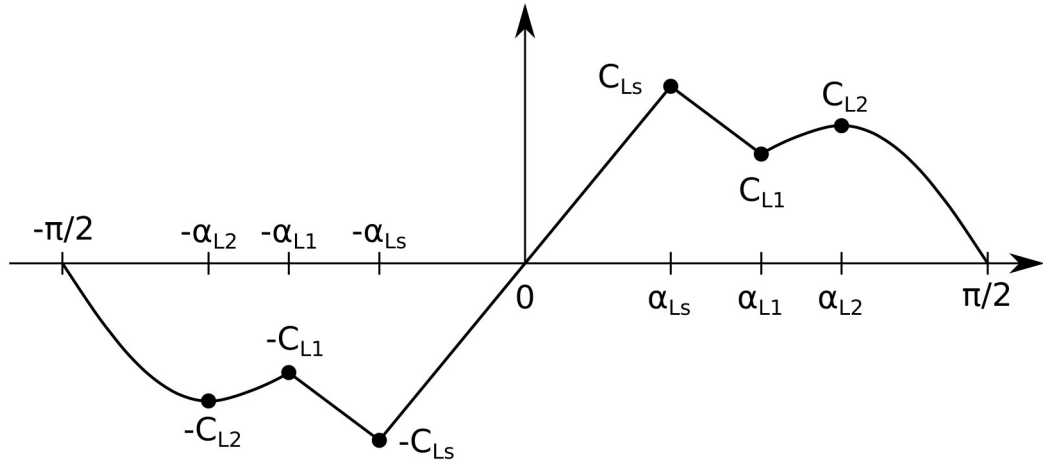


Figure 2-1: Lift coefficient approximation

Lift coefficient is given by the following expressions.

$$C_L = \frac{-(\alpha + \alpha_{L2})\left(\alpha + \frac{\pi}{2}\right)}{(\alpha_{L1} - \alpha_{L2})\left(\alpha_{L1} - \frac{\pi}{2}\right)} C_{L1} - \frac{(\alpha + \alpha_{L1})\left(\alpha + \frac{\pi}{2}\right)}{(\alpha_{L2} - \alpha_{L1})\left(\alpha_{L2} - \frac{\pi}{2}\right)} C_{L2}, \text{ for } -\frac{\pi}{2} \leq \alpha \leq -\alpha_{L1} \quad (2.1)$$

$$C_L = \frac{C_{L1} - C_{Ls}}{\alpha_{L1} - \alpha_{Ls}} (\alpha + \alpha_{Ls}) - C_{Ls}, \text{ for } -\alpha_{L1} < \alpha \leq -\alpha_{Ls} \quad (2.2)$$

$$C_L = \frac{C_{Ls}}{\alpha_{Ls}} \alpha, \text{ for } -\alpha_{Ls} < \alpha < \alpha_{Ls} \quad (2.3)$$

$$C_L = \frac{C_{L1} - C_{Ls}}{\alpha_{L1} - \alpha_{Ls}} (\alpha - \alpha_{Ls}) + C_{Ls}, \text{ for } \alpha_{Ls} \leq \alpha < \alpha_{L1} \quad (2.4)$$

$$C_L = \frac{(\alpha - \alpha_{L2})\left(\alpha - \frac{\pi}{2}\right)}{(\alpha_{L1} - \alpha_{L2})\left(\alpha_{L1} - \frac{\pi}{2}\right)} C_{L1} + \frac{(\alpha - \alpha_{L1})\left(\alpha - \frac{\pi}{2}\right)}{(\alpha_{L2} - \alpha_{L1})\left(\alpha_{L2} - \frac{\pi}{2}\right)} C_{L2}, \text{ for } \alpha_{L1} \leq \alpha \leq \frac{\pi}{2} \quad (2.5)$$

Following approximation is used to get drag coefficient for the full range of angle of attack. [4]  
 Drag coefficient is assumed to be symmetric.

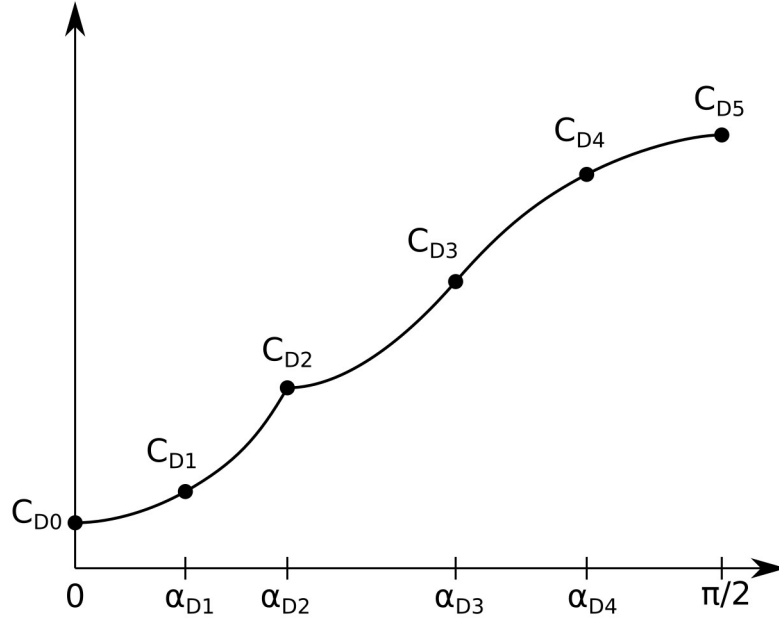


Figure 2-2: Drag coefficient approximation

Drag coefficient is given by the following expressions.

$$C_D = \frac{(\alpha^2 - \alpha_{D2}^2)(\alpha^2 - \alpha_{D1}^2)}{\alpha_{D1}^2 \alpha_{D2}^2} C_{D0} + \frac{(\alpha^2 - \alpha_{D2}^2) \alpha^2}{(\alpha_{D1}^2 - \alpha_{D2}^2) \alpha_{D1}^2} C_{D1} + \frac{(\alpha^2 - \alpha_{D1}^2) \alpha^2}{(\alpha_{D2}^2 - \alpha_{D1}^2) \alpha_{D2}^2} C_{D2}, \quad (2.6)$$

for  $-\alpha_{D2} \leq \alpha \leq \alpha_{D2}$

$$C_D = \frac{(\alpha - \alpha_{D3})(\alpha - \alpha_{D4}) \left( \alpha - \frac{\pi}{2} \right)}{(\alpha_{D2} - \alpha_{D3})(\alpha_{D2} - \alpha_{D4}) \left( \alpha_{D2} - \frac{\pi}{2} \right)} C_{D2} + \frac{(\alpha - \alpha_{D2})(\alpha - \alpha_{D4}) \left( \alpha - \frac{\pi}{2} \right)}{(\alpha_{D3} - \alpha_{D2})(\alpha_{D3} - \alpha_{D4}) \left( \alpha_{D3} - \frac{\pi}{2} \right)} C_{D3} \\ + \frac{(\alpha - \alpha_{D2})(\alpha - \alpha_{D3}) \left( \alpha - \frac{\pi}{2} \right)}{(\alpha_{D4} - \alpha_{D2})(\alpha_{D4} - \alpha_{D3}) \left( \alpha_{D4} - \frac{\pi}{2} \right)} + C_{D4} \frac{(\alpha - \alpha_{D2})(\alpha - \alpha_{D3})(\alpha - \alpha_{D4})}{\left( \frac{\pi}{2} - \alpha_{D2} \right) \left( \frac{\pi}{2} - \alpha_{D3} \right) \left( \frac{\pi}{2} - \alpha_{D4} \right)} C_{D5}, \quad (2.7)$$

for  $-\alpha_{D2} \leq \alpha \leq \alpha_{D2}$

Data available in [5] and [6] can be used to approximate aerodynamic characteristics outside linear range of the lift.

## 2.2. Finite Wing Aerodynamic Characteristics

Aerodynamic characteristics of the finite wing can be estimated within linear range of the lift.

Lift curve slope is given as follows. [7]

$$\frac{dC_L}{d\alpha} = \frac{2\pi A}{2 + \sqrt{4 + A^2} (1 + \tan^2(\Lambda_{t/c}))} \quad (2.8)$$

The finite wing lift coefficient within linear range is given by the following formula. [7]

$$C_L = C_{L\alpha=0} + \frac{dC_L}{d\alpha} \alpha \quad (2.9)$$

The finite wing maximum lift coefficient is given by. [1]

$$C_{Lmax} = 0.9 C_{Lmax\infty} \cos \Lambda_{t/c} \quad (2.10)$$

The finite wing drag coefficient is given as follows. [7]

$$C_D = C_{D0} + \frac{C_L^2}{\pi A e} \quad (2.11)$$

## 2.3. Horizontal Tail Incidence

Equilibrium of moments acting on an aircraft is given by the following equation.

$$r_{CG} mg + \frac{1}{2} \rho V^2 S \hat{C}_m = l_h \frac{1}{2} \rho V^2 S_h C_{L,h} \quad (2.12)$$

Horizontal stabilizer lift coefficient is given as follows.

$$C_{L,h} = \left( \alpha + i_h - \alpha \frac{\partial \epsilon}{\partial \alpha} \right) \frac{dC_{L,h}}{d\alpha} \quad (2.13)$$

where downwash derivative is given as

$$\frac{\partial \epsilon}{\partial \alpha} = \frac{2a}{\pi \Lambda} \quad (2.14)$$

Substituting equation (2.13) into (2.12) gives

$$r_{CG} mg + \frac{1}{2} \rho V^2 S \hat{C}_m = l_h \frac{1}{2} \rho V^2 S_h \left( \alpha + i_h - \alpha \frac{\partial \epsilon}{\partial \alpha} \right) \frac{dC_{L,h}}{d\alpha} \quad (2.15)$$

Solving this equation for horizontal tail incidence angle gives

$$i_h = \frac{2r_{CG} mg + \rho V^2 S \hat{C}_m}{l_h \rho V^2 S_h \frac{dC_{L,h}}{d\alpha}} - \alpha \left( 1 - \frac{\partial \epsilon}{\partial \alpha} \right) \quad (2.16)$$

Equilibrium of forces acting on an aircraft in level flight is given by the following equation.

$$mg = \frac{1}{2} \rho V^2 S C_L \quad (2.17)$$

Aircraft lift coefficient is given as follows.

$$C_L = C_{L0} + \alpha \frac{dC_L}{d\alpha} \quad (2.18)$$

Substituting equation (2.18) into (2.17) gives

$$mg = \frac{1}{2} \rho V^2 S \left( C_{L0} + \alpha \frac{dC_L}{d\alpha} \right) \quad (2.19)$$

Solving this equation for angle of attack gives

$$\alpha = \frac{2mg - \rho V^2 S C_{L0}}{\rho V^2 S \frac{dC_L}{d\alpha}} \quad (2.20)$$

Substituting equation (2.20) into (2.16) gives

$$i_h = \frac{2r_{CG}mg + \rho V^2 S \hat{C}_m}{l_h \rho V^2 S_h \frac{dC_{L,h}}{d\alpha}} - \frac{2mg - \rho V^2 S C_{L0}}{\rho V^2 S \frac{dC_L}{d\alpha}} \left( 1 - \frac{\partial \epsilon}{\partial \alpha} \right) \quad (2.21)$$

## 2.4. Critical Angle of Attack

Equilibrium of forces acting on an aircraft in level flight is given by the following equation.

$$mg = \frac{1}{2} \rho V^2 (S C_L + S_h C_{L,h}) \quad (2.22)$$

As conventional configuration airplanes have horizontal stabilizer negative incidence angle, it is assumed that horizontal stabilizer is within its lift linear range when maximum lift coefficient is reached.

$$mg = \frac{1}{2} \rho V^2 \left[ S C_L + S_h \left( \alpha_{cr} + i_h - \alpha_{cr} \frac{\partial \epsilon}{\partial \alpha} \right) \frac{dC_{L,h}}{d\alpha} \right] \quad (2.23)$$

Solving this equation for the maximum lift coefficient gives

$$C_{L,max} = \frac{mg - \frac{1}{2} \rho V_{stall}^2 S_h \left( \alpha_{cr} + i_h - \alpha_{cr} \frac{\partial \epsilon}{\partial \alpha} \right) \frac{dC_{L,h}}{d\alpha}}{\frac{1}{2} \rho V_{stall}^2 S} \quad (2.24)$$

Assuming that maximum lift coefficient is within linear range, then critical angle of attack is given as follows.

$$C_{L,max} = C_{L0} + \alpha_{cr} \frac{dC_L}{d\alpha} \quad (2.25)$$

Substituting equation (2.25) into (2.24) gives

$$C_{L0} + \alpha_{cr} \frac{dC_L}{d\alpha} = \frac{mg - \frac{1}{2} \rho V_{stall}^2 S_h \left( \alpha_{cr} + i_h - \alpha_{cr} \frac{\partial \epsilon}{\partial \alpha} \right) \frac{dC_{L,h}}{d\alpha}}{\frac{1}{2} \rho V_{stall}^2 S} \quad (2.26)$$

Solving this equation for critical angle of attack gives

$$\alpha_{cr} = \frac{2mg - \rho V_{stall}^2 \left( S_h i_h \frac{dC_{L,h}}{d\alpha} + S C_{L0} \right)}{\rho V_{stall}^2 \left[ S \frac{dC_L}{d\alpha} + S_h \left( 1 - \frac{\partial \epsilon}{\partial \alpha} \right) \frac{dC_{L,h}}{d\alpha} \right]} \quad (2.27)$$

## **3. Mass and Inertia Data**

### **3.1. Structure Groups Breakdown**

Inertia tensor and center of mass coordinates can be estimated by breaking down empty aircraft into structure groups and then estimating their weights, inertia moments and coordinates, e.g. using aircraft drawing. [3]

### **3.2. OpenVSP**

Mass Properties tool of the OpenVSP can be used to compute aircraft center of mass position and inertia tensor.

## 4. Computational Fluid Dynamics

### 4.1. Tools

#### 4.1.1. XFOIL

XFOIL is a program for the analysis of subsonic isolated airfoils developed at the Massachusetts Institute of Technology.

#### 4.1.2. VSPAERO

VSPAERO is a combined vortex lattice method (VLM) and panel method solver integrated with OpenVSP, a parametric aircraft geometry tool developed at NASA Ames Research Center. VSPAERO can be used to compute aircraft aerodynamic characteristics within linear range of the lift. [8] OpenVSP allows users to fast create an aircraft 3D model by defining geometric parameters.

#### 4.1.3. OpenFOAM

OpenFOAM is an open source software for computational fluid dynamics (CFD) originally created at Imperial College London. OpenFOAM contains various solvers intended to simulate different physical phenomena.

### 4.2. Workflow

#### 4.2.1. XFOIL

Follow this steps to obtain airfoil characteristics. Notice that XFOIL commands are case sensitive. [9]

1. Open terminal and execute `xfoil` program.  
XFOIL command prompt should start.
2. Read buffer airfoil from coordinate file with `LOAD` command e.g `LOAD 2412.dat`,  
or set NACA 4 or 5 digit airfoil with `NACA` command e.g. `NACA 2412`.  
Coordinate file is a simple text file which contains list of the 2D airfoil coordinate points starting at the trailing edge, progressing to the leading edge along the upper surface, and returning to the trailing edge along the lower surface.
3. Set number of panel nodes to at least 160 with `PPAR` command if necessary.

4. Enter operation mode with **OPER** command. **OPERi** indicates inviscid mode.
5. Enter viscous mode with **ViSC** command.  
Enter Reynolds number for typical flight conditions. **OPERV** should be displayed.
6. Set Mach number for typical flight conditions with **Mach** command.
7. Specify output files with **PACC** command.
8. Specify the angle of attack range and run computations with **Aseq** command.

#### 4.2.2. VSPAERO

An appropriately define aircraft 3D model is needed to analyze. [10] Based on this model degenerated geometry file is generated for the vortex lattice method and surface triangulation file for the panel method.

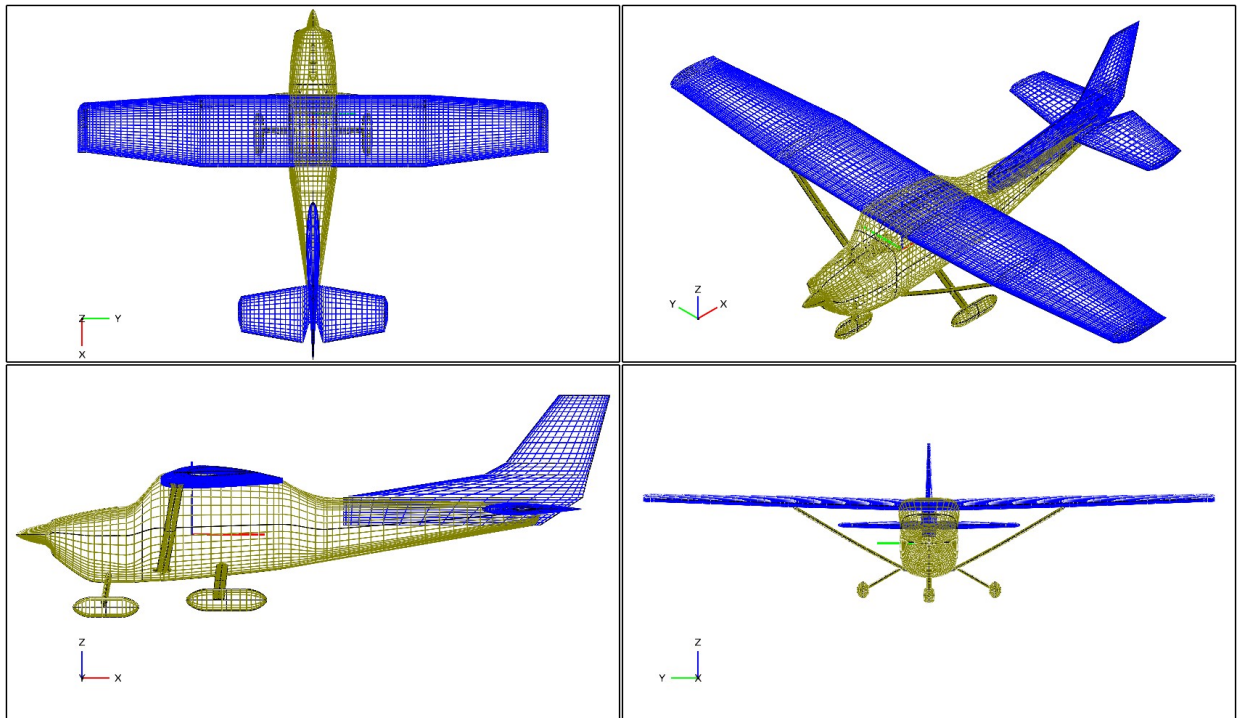


*Figure 4-1: OpenVSP aircraft model*

VSPAERO can be run from within Analysis menu of the OpenVSP. Some additional setup should be done to start computations. Vortex lattice method or panel method solver should be chosen. Reference area, lengths and moment reference position should be specified to get correct results. Angle of attack range should be specified for the linear range of the lift. Critical angle of attack can be calculated using formula (2.27). Mach number should be set to typical flight conditions.



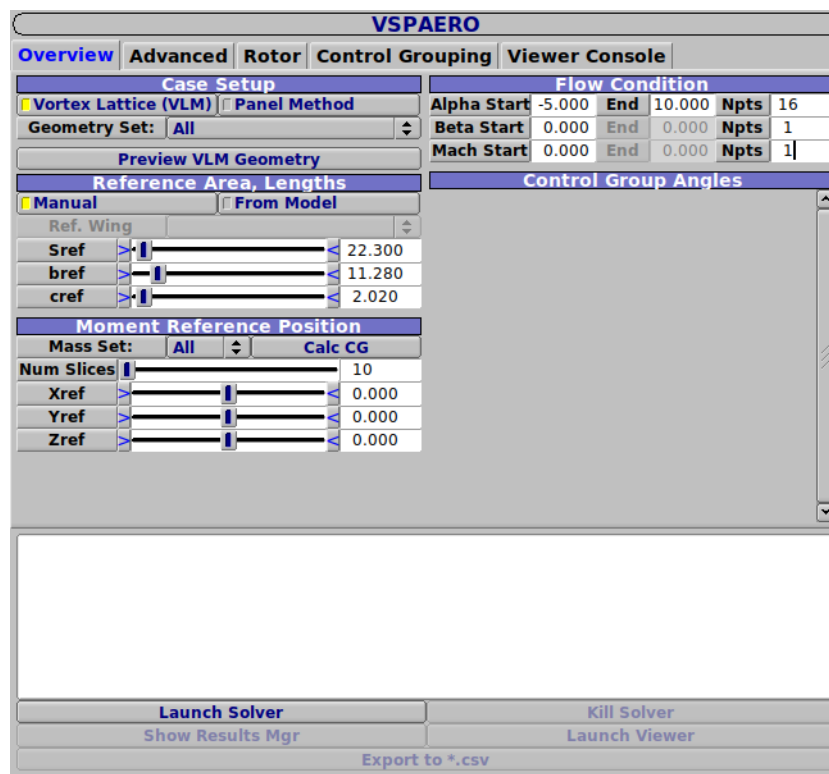


Figure 4-2: VSPAERO computations setup window

VSPAERO Viewer and Results Manager can be used to visualize results. Computed aerodynamic characteristics are saved as plain text files, which are both easy to understand by a human and easy to read by a computer program.

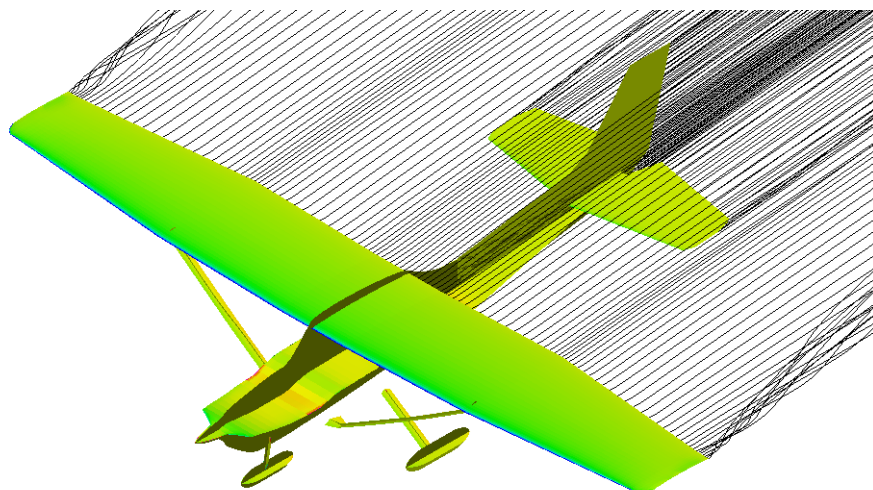


Figure 4-3: Wakes and pressure coefficient change distribution

### 4.2.3. OpenFOAM

#### Solver

OpenFOAM `simpleFoam` is a steady-state solver for incompressible, turbulent flow using SIMPLE (Semi-Implicit Method for Pressure Linked Equations) algorithm, which can be used to compute aircraft aerodynamic characteristics for the full range of angle of attack. [11], [12], [13]

SST  $k-\omega$  Reynolds-Averaged Navier-Stokes (RANS) turbulence model is used.

#### Mesh – Control Volume

OpenFOAM `blockMesh` utility is used to create control volume mesh defined in `system/blockMeshDict` dictionary file as a mesh composed of hexahedral blocks.

The simplest case is when the control volume is defined by exactly one rectangular prisms.

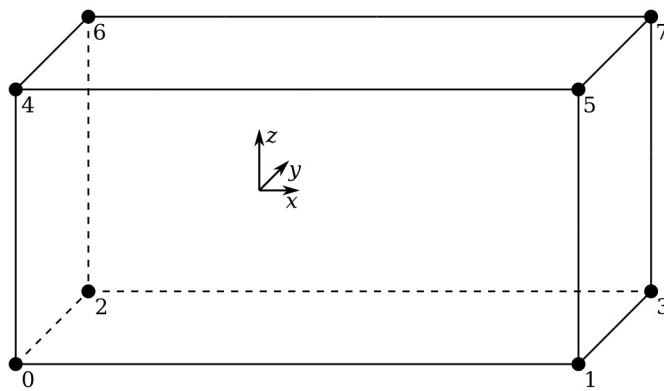


*Figure 4-4: Basic control volume scheme*

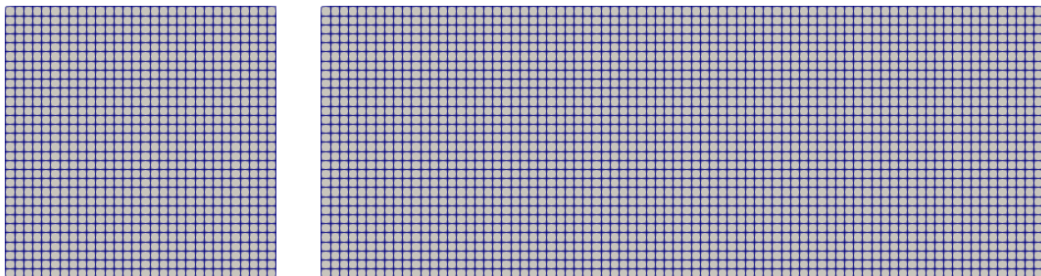


*Figure 4-5: Basic control volume mesh*

Dictionary file is listed below.

```

/*-----* C++ *-----*\
|=====|
|  \ \ /  F ield      | OpenFOAM: The Open Source CFD Toolbox
|  \ \ /  O peration  | Version: 6
|  \ \ /  A nd        | Web: www.OpenFOAM.org
|  \ \ /  M anipulation|
\*-----*/
FoamFile
{
    version      2.0;
    format       ascii;
    class        dictionary;
    object       blockMeshDict;
}
// * * * * * //

cv_x_min -20.0;
cv_x_max  60.0;
cv_y_min -15.0;
cv_y_max  15.0;
cv_z_min -15.0;
cv_z_max  15.0;

convertToMeters 1.0;

vertices
(
    ( $cv_x_min $cv_y_min $cv_z_min )
    ( $cv_x_max $cv_y_min $cv_z_min )
    ( $cv_x_min $cv_y_max $cv_z_min )
    ( $cv_x_max $cv_y_max $cv_z_min )
    ( $cv_x_min $cv_y_min $cv_z_max )
    ( $cv_x_max $cv_y_min $cv_z_max )
    ( $cv_x_min $cv_y_max $cv_z_max )
    ( $cv_x_max $cv_y_max $cv_z_max )
);

blocks
(
    hex ( 0 1 3 2 4 5 7 6 ) ( 80 30 30 ) simpleGrading ( 1 1 1 )
);

edges
(
);

boundary
(
    inlet
    {
        type patch;
        faces
        (
            ( 0 4 6 2 )
        );
    }
);

```

```

outlet
{
    type patch;
    faces
    (
        ( 1 3 7 5 )
    );
}

walls
{
    type patch;
    faces
    (
        ( 0 1 5 4 ) // left
        ( 2 6 7 3 ) // right
        ( 0 2 3 1 ) // bottom
        ( 4 5 7 6 ) // top
    );
}

);

mergePatchPairs
(
);

```

## Mesh – Simple Grading

Grading is used to increase mesh resolution in regions of interest. Due to create graded control volume mesh it has to be divided into subdomains. Scheme of control volume mesh one dimension grading is presented below.

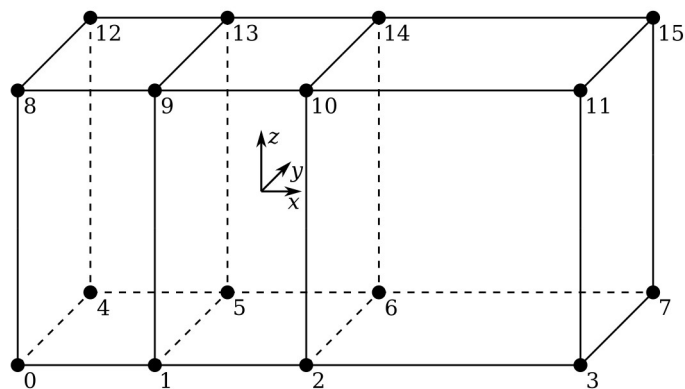


Figure 4-6: Graded control volume scheme

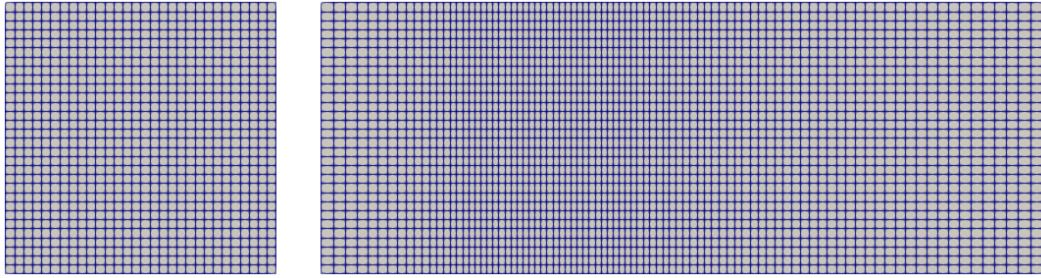


Figure 4-7: Graded control volume mesh

Dictionary file is listed below.

```

/*-----*- C++ -*-----*\
|=====|
|  \ \  /  F ield      | OpenFOAM: The Open Source CFD Toolbox
|  \ \  /  O peration  | Version: 6
|  \ \  /  A nd        | Web:      www.OpenFOAM.org
|  \ \  /  M anipulation|
|-----*\
FoamFile
{
    version      2.0;
    format       ascii;
    class        dictionary;
    object       blockMeshDict;
}
// * * * * *

cv_x_min -20.0;
cv_x_max  60.0;
cv_y_min -15.0;
cv_y_max  15.0;
cv_z_min -15.0;
cv_z_max  15.0;
s2_x_min  -5.0;
s2_x_max  15.0;

convertToMeters 1.0;

vertices
(
    ( $cv_x_min $cv_y_min $cv_z_min )
    ( $s2_x_min $cv_y_min $cv_z_min )
    ( $s2_x_max $cv_y_min $cv_z_min )
    ( $cv_x_max $cv_y_min $cv_z_min )
    ( $cv_x_min $cv_y_max $cv_z_min )
    ( $s2_x_min $cv_y_max $cv_z_min )
    ( $s2_x_max $cv_y_max $cv_z_min )
    ( $cv_x_max $cv_y_max $cv_z_min )
    ( $cv_x_min $cv_y_min $cv_z_max )
    ( $s2_x_min $cv_y_min $cv_z_max )
    ( $s2_x_max $cv_y_min $cv_z_max )
    ( $cv_x_max $cv_y_min $cv_z_max )
    ( $cv_x_min $cv_y_max $cv_z_max )
    ( $s2_x_min $cv_y_max $cv_z_max )
)

```

```

( $s2_x_max $cv_y_max $cv_z_max )
( $cv_x_max $cv_y_max $cv_z_max )
);

blocks
(
    hex ( 0 1 5 4 8 9 13 12 ) ( 15 30 30 ) simpleGrading ( 0.5 1.0 1.0 )
    hex ( 1 2 6 5 9 10 14 13 ) ( 30 30 30 ) simpleGrading ( 1.0 1.0 1.0 )
    hex ( 2 3 7 6 10 11 15 14 ) ( 45 30 30 ) simpleGrading ( 2.0 1.0 1.0 )
);

edges
(
);

boundary
(
    inlet
    {
        type patch;
        faces
        (
            ( 0 8 12 4 )
        );
    }

    outlet
    {
        type patch;
        faces
        (
            ( 3 7 15 11 )
        );
    }

    walls
    {
        type patch;
        faces
        (
            // left
            ( 0 1 9 8 )
            ( 1 2 10 9 )
            ( 2 3 11 10 )
            // right
            ( 4 12 13 5 )
            ( 5 13 14 6 )
            ( 6 14 15 7 )
            // bottom
            ( 0 4 5 1 )
            ( 1 5 6 2 )
            ( 2 6 7 3 )
            // top
            ( 8 9 13 12 )
            ( 9 10 14 13 )
            ( 10 11 15 14 )
        );
    }
);

```

```
mergePatchPairs
(
);
```

## Mesh – Complex Grading

Scheme of complex control volume mesh grading is presented below.

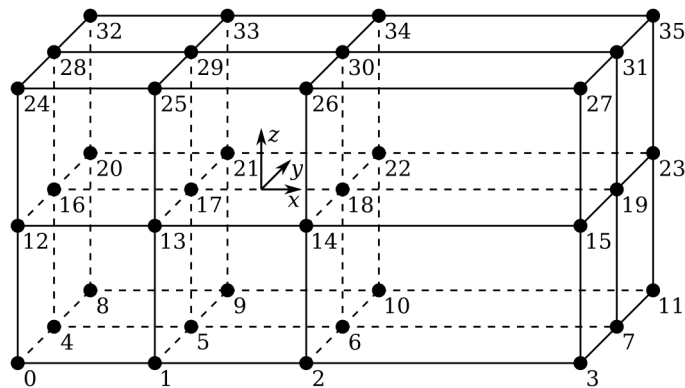


Figure 4-8: Complex graded control volume scheme

For symmetric cases only half of the geometry can be considered to reduce computation time.

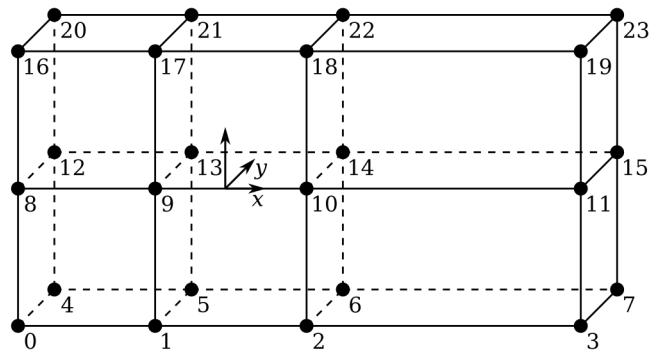


Figure 4-9: Symmetric control volume scheme

Dictionary file is listed below.

```
/*----- C++ -----*/
|=====|
| \ \ / | F ield      | OpenFOAM: The Open Source CFD Toolbox
| \ \ / | O peration  | Version: 6
| \ \ / | A nd        | Web:      www.OpenFOAM.org
| \ \ / | M anipulation|
/*-----*/
```

```

FoamFile
{
    version      2.0;
    format       ascii;
    class        dictionary;
    object       blockMeshDict;
}
// * * * * *

cv_x_min -20.0;
cv_x_max  60.0;
cv_y_min -15.0;
cv_y_max  15.0;
cv_z_min -15.0;
cv_z_max  15.0;

s2_x_min  -5.0;
s2_x_max  15.0;

convertToMeters 1.0;

vertices
(
    ( $cv_x_min      0.0 $cv_z_min )
    ( $s2_x_min      0.0 $cv_z_min )
    ( $s2_x_max      0.0 $cv_z_min )
    ( $cv_x_max      0.0 $cv_z_min )
    ( $cv_x_min $cv_y_max $cv_z_min )
    ( $s2_x_min $cv_y_max $cv_z_min )
    ( $s2_x_max $cv_y_max $cv_z_min )
    ( $cv_x_max $cv_y_max $cv_z_min )
    ( $cv_x_min      0.0      0.0 )
    ( $s2_x_min      0.0      0.0 )
    ( $s2_x_max      0.0      0.0 )
    ( $cv_x_max      0.0      0.0 )
    ( $cv_x_min $cv_y_max      0.0 )
    ( $s2_x_min $cv_y_max      0.0 )
    ( $s2_x_max $cv_y_max      0.0 )
    ( $cv_x_max $cv_y_max      0.0 )
    ( $cv_x_min      0.0 $cv_z_max )
    ( $s2_x_min      0.0 $cv_z_max )
    ( $s2_x_max      0.0 $cv_z_max )
    ( $cv_x_max      0.0 $cv_z_max )
    ( $cv_x_min $cv_y_max $cv_z_max )
    ( $s2_x_min $cv_y_max $cv_z_max )
    ( $s2_x_max $cv_y_max $cv_z_max )
    ( $cv_x_max $cv_y_max $cv_z_max )
);

blocks
(
    hex ( 0 1 5 4 8 9 13 12 ) ( 15 15 15 ) simpleGrading ( 0.5 2.0 0.5 )
    hex ( 8 9 13 12 16 17 21 20 ) ( 15 15 15 ) simpleGrading ( 0.5 2.0 2.0 )
    hex ( 1 2 6 5 9 10 14 13 ) ( 30 15 15 ) simpleGrading ( 1.0 2.0 0.5 )
    hex ( 9 10 14 13 17 18 22 21 ) ( 30 15 15 ) simpleGrading ( 1.0 2.0 2.0 )
    hex ( 2 3 7 6 10 11 15 14 ) ( 45 15 15 ) simpleGrading ( 2.0 2.0 0.5 )
    hex ( 10 11 15 14 18 19 23 22 ) ( 45 15 15 ) simpleGrading ( 2.0 2.0 2.0 )
);

```



```
edges
(
);

boundary
(
    inlet
    {
        type patch;
        faces
        (
            ( 0 8 12 4 )
            ( 8 16 20 12 )
        );
    }

    outlet
    {
        type patch;
        faces
        (
            ( 3 7 15 11 )
            ( 11 15 23 19 )
        );
    }

    sym
    {
        type symmetryPlane;
        faces
        (
            // left
            ( 0 1 9 8 )
            ( 8 9 17 16 )
            ( 1 2 10 9 )
            ( 9 10 18 17 )
            ( 2 3 11 10 )
            ( 10 11 19 18 )
        );
    }

    walls
    {
        type patch;
        faces
        (
            // right
            ( 4 12 13 5 )
            ( 12 20 21 13 )
            ( 5 13 14 6 )
            ( 13 21 22 14 )
            ( 6 14 15 7 )
            ( 14 22 23 15 )

            // bottom
            ( 0 4 5 1 )
            ( 1 5 6 2 )
            ( 2 6 7 3 )
        );
    }
}
```

```
        // top
        ( 16 17 21 20 )
        ( 17 18 22 21 )
        ( 18 19 23 22 )
    );
}
);
mergePatchPairs
(
);
```

## Mesh – Aircraft Geometry Model

OpenVSP can be used to create aircraft 3D model and export it to STL. OpenFOAM `snappyHexMesh` utility is used to combine control volume mesh with aircraft geometry model. Volume near aircraft geometry can be refined due to achieve better results. Meshing parameters are specified in `system/snappyHexMeshDict` file.

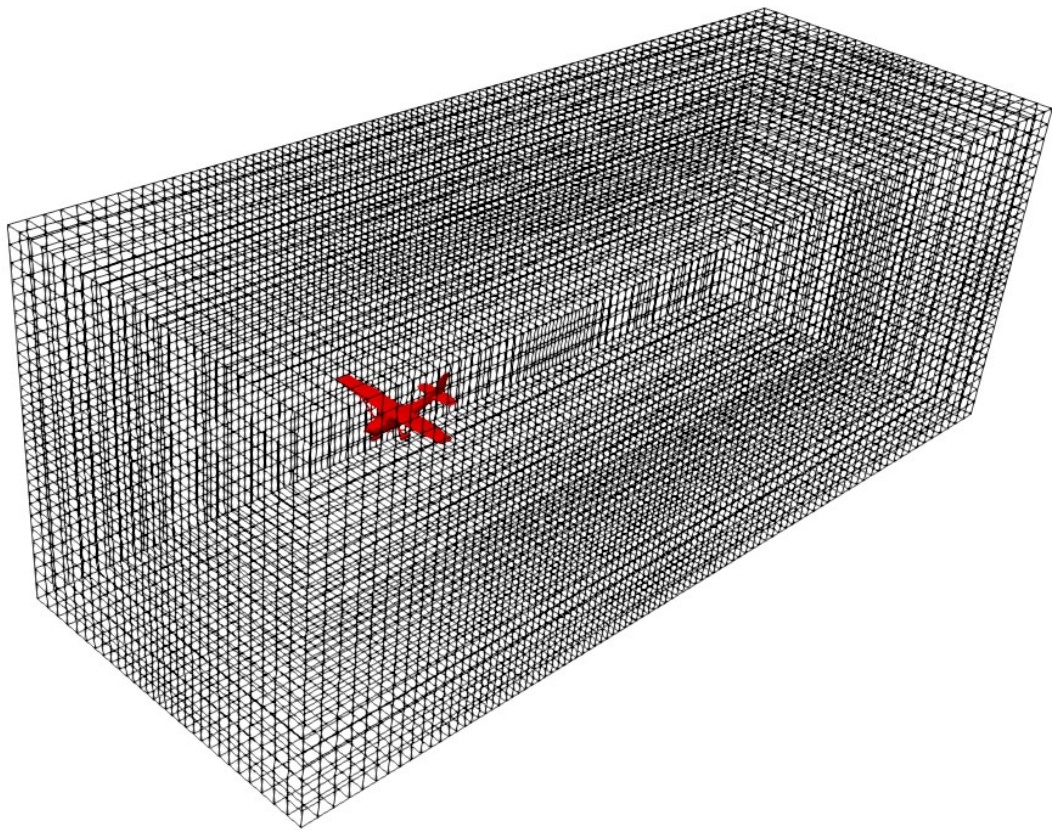


*Figure 4-10: OpenFOAM complete mesh*

## Initial and Boundary Conditions

The inlet boundary conditions are given as follows. [14]

$$k = \frac{3}{2} (I V)^2 \quad (4.1)$$

$$\omega = \frac{k^{0.5}}{C_\mu L} \quad (4.2)$$

where: [12], [13], [15], [16], [17]

$$I = 0.16 \text{Re}^{-1/8} \quad (4.3)$$

$$C_\mu = 0.09 \quad (4.4)$$

## Control

Notice that, as this is a steady-state simulation, time should be treated rather as iteration parameter rather than as a physical time. Maximum number of iterations in set `system/controlDict` dictionary file, `endTime` is a maximum number of iterations when `deltaT` is 1.

## Solution

Case solving is terminated when pressure, velocity, turbulent kinetic energy and specific turbulence dissipation rate initial residual of the field equations falls below threshold values defined in `residualControl` dictionary in `system/fvSolution` file.

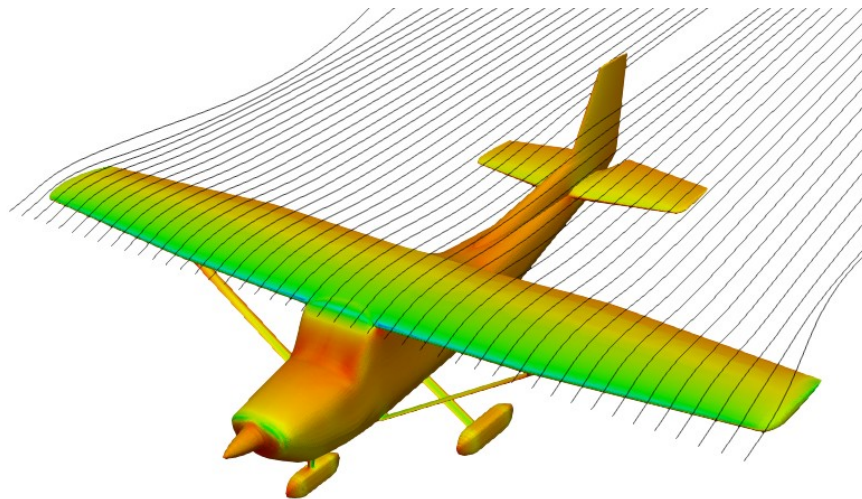


*Figure 4-11: Streamlines and kinematic pressure distribution*

If divergent or unstable behavior is observed decreasing under-relaxation factors defined in `relaxationFactors` dictionary in `system/fvSolution` file may improve solution convergence.

Physical quantity	Under-Relaxation Factor
Kinematic pressure	0.2 – 0.3
Velocity	0.5 – 0.7
Turbulent kinetic energy	0.5 – 0.7
Turbulence dissipation rate	0.5 – 0.7

Table 4-1: Commonly used under-relaxation factors [17], [18]

## 4.3. Results

### 4.3.1. XFOIL

XFOIL computations results, compared to the data available in [5] and [6], are shown in the following figures.

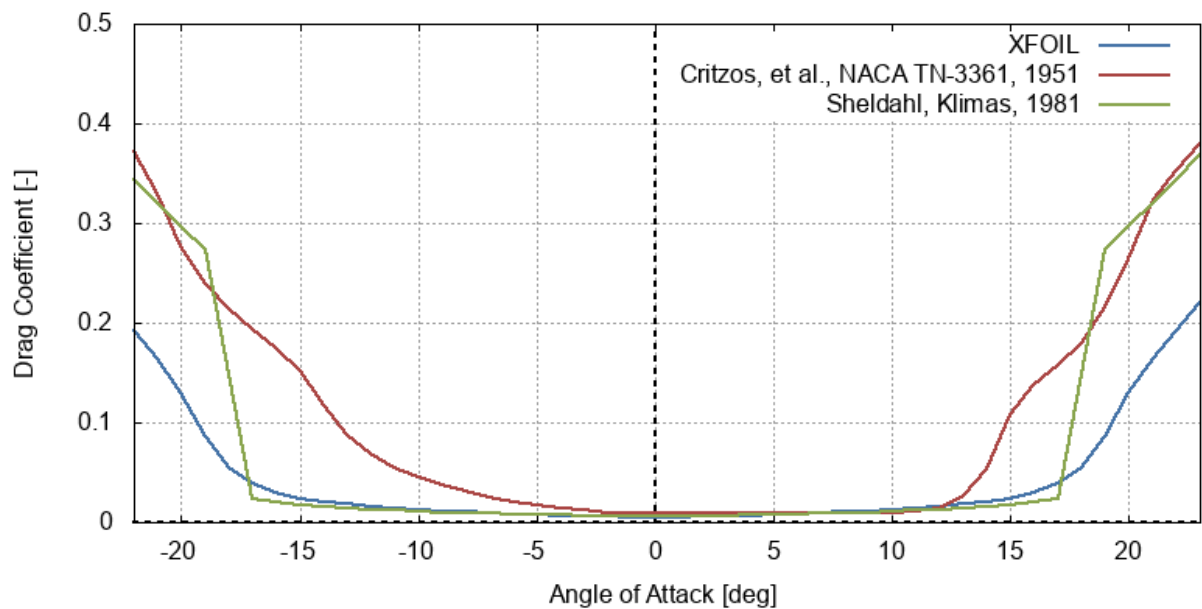


Figure 4-12: NACA 0012 airfoil drag coefficient

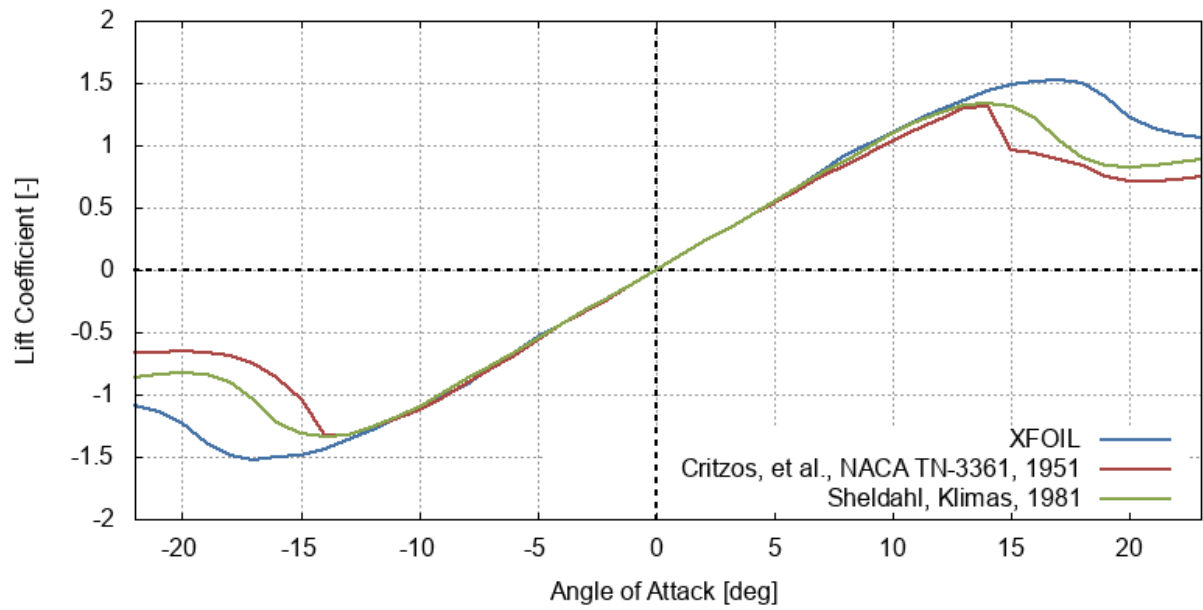


Figure 4-13: NACA 0012 airfoil lift coefficient

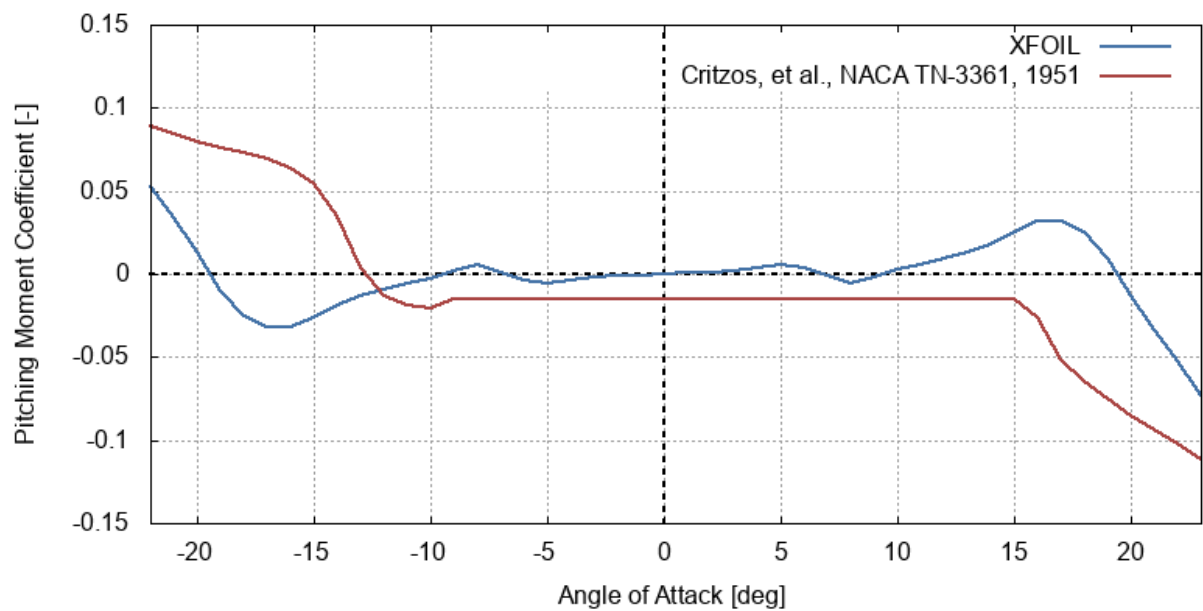


Figure 4-14: NACA 0012 airfoil pitching moment coefficient

### 4.3.2. VSPAERO

VSPAERO computations results, compared to the OpenFOAM computations results, are shown in the following figures.

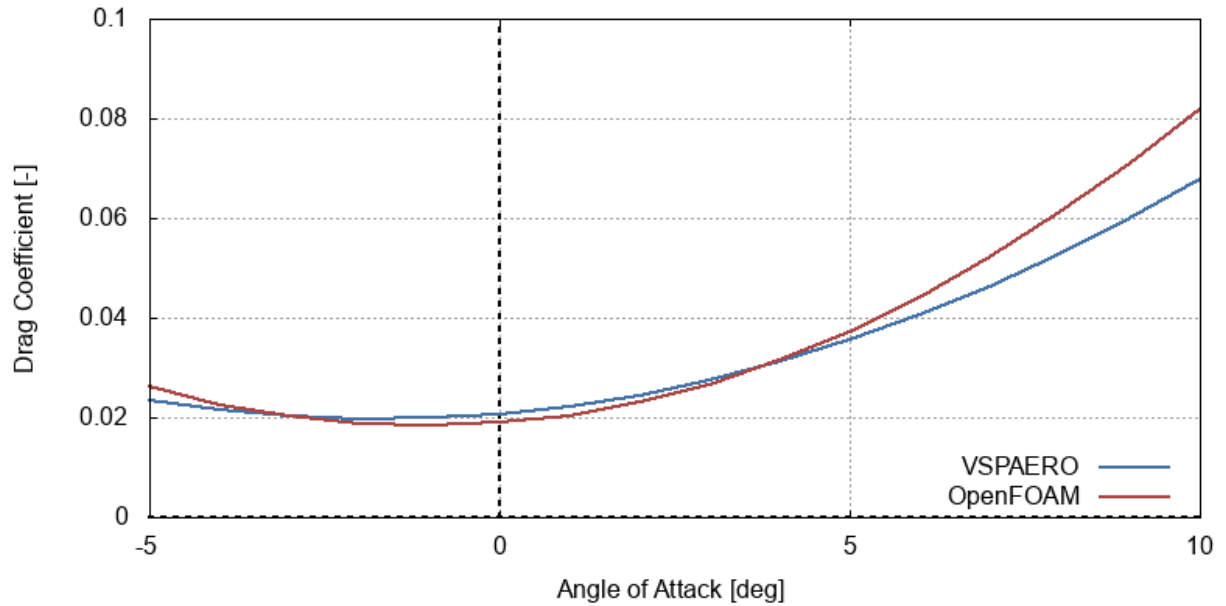


Figure 4-15: Drag coefficient

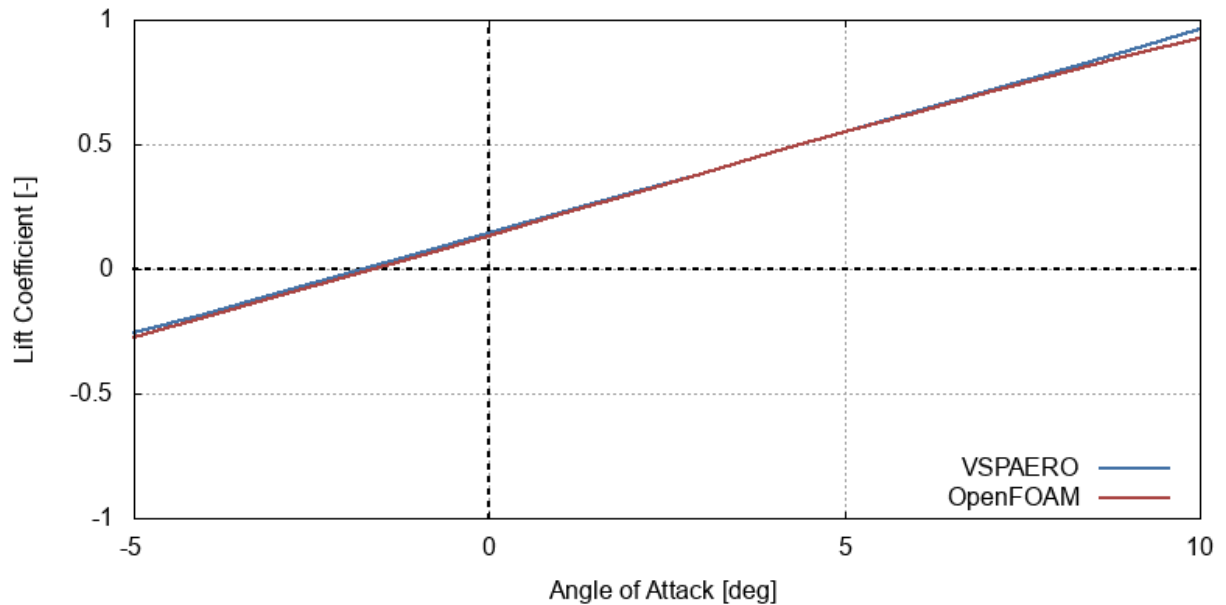


Figure 4-16: Lift coefficient

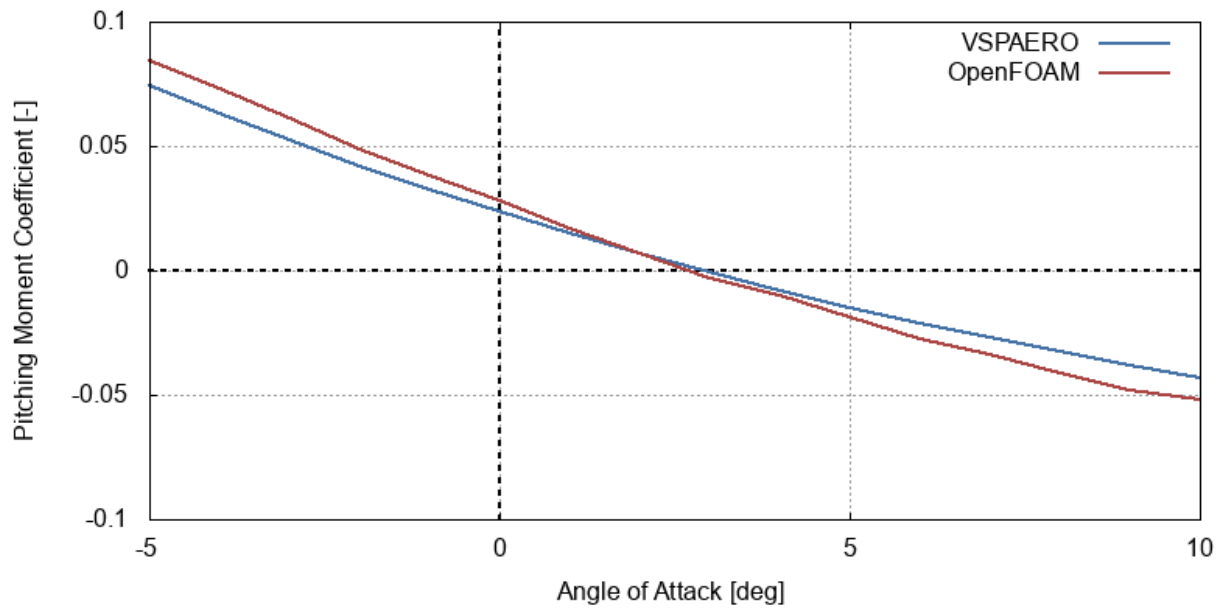


Figure 4-17: Pitching moment coefficient

#### 4.3.3. OpenFOAM

OpenFOAM computations results, compared to the data available in [19], are shown in the following figures.

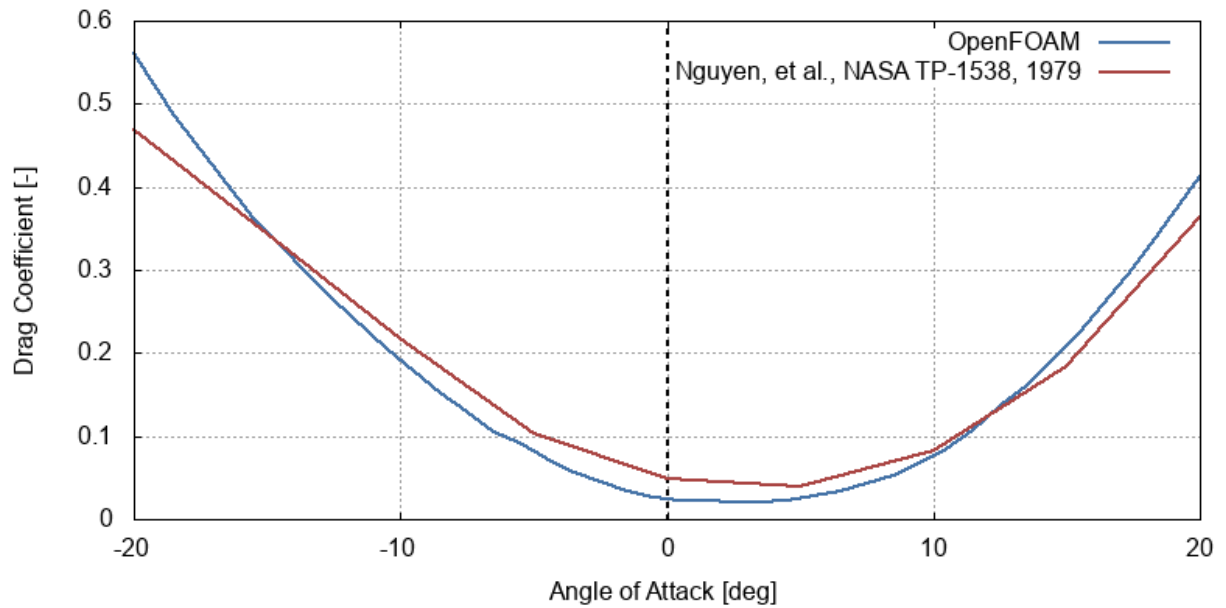


Figure 4-18: F-16 drag coefficient

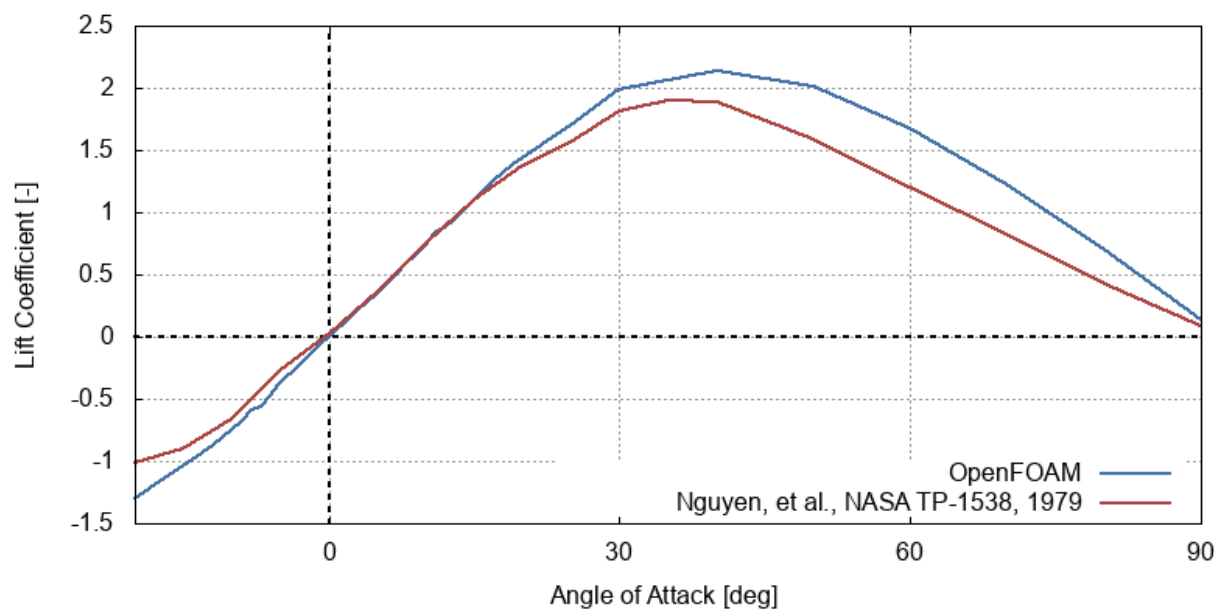


Figure 4-19: F-16 lift coefficient



## Bibliography

- [1] Raymer D.: Aircraft Design: A Conceptual Approach. American Institute of Aeronautics and Astronautics, 1992
- [2] Galiński C.: Wybrane zagadnienia projektowania samolotów. Wydawnictwa Naukowe Instytutu Lotnictwa, 2016 [in Polish]
- [3] Torenbeek E.: Synthesis of Subsonic Airplane Design. Delft University Press, 1982
- [4] Takahashi M.: A Flight-Dynamic Helicopter Mathematical Model with a Single Flap-Lag-Torsion Main Rotor. National Aeronautics and Space Administration, TM-102267, 1990
- [5] Critzos C., et al.: Aerodynamic Characteristics of NACA 0012 Airfoil Sections at Angles of Attack from 0 to 180. National Advisory Committee for Aeronautics, TN-3361, 1955
- [6] Sheldahl R., Klimas P.: Aerodynamic Characteristics of Seven Symmetrical Airfoil Sections Through 180-Degree Angle of Attack for Use in Aerodynamic Analysis of Vertical Axis Wind Turbines. Sandia National Laboratories, 1981
- [7] Corke T.: Design of Aircraft. Pearson Education, 2003
- [8] Litherland B.: Using VSPAERO. [online]. 2015 [Accessed 2019-01-20]. Available from: <http://openvsp.org/wiki/doku.php?id=vspaerotutorial>
- [9] Drela M., Youngren H.: XFOIL 6.9 User Primer. [online]. 2001 [Accessed 2019-01-20]. Available from: [https://web.mit.edu/drela/Public/web/xfoil/xfoil\\_doc.txt](https://web.mit.edu/drela/Public/web/xfoil/xfoil_doc.txt)
- [10] Litherland B.: Modeling for VSPAERO. [online]. 2015 [Accessed 2019-05-12]. Available from: <http://openvsp.org/wiki/doku.php?id=vspaeromodeling>
- [11] Greenshields C.: OpenFOAM User Guide version 6. OpenFOAM Foundation Ltd., 2018
- [12] Moukalled F., Mangani L., Darwish M.: The Finite Volume Method in Computational Fluid Dynamics, An Advanced Introduction with OpenFOAM and Matlab. Springer International Publishing, 2016
- [13] Versteeg H., Malalasekera W.: An Introduction to Computational Fluid Dynamics, The Finite Volume Method. Pearson Education Limited, 2007
- [14] OpenFOAM: User Guide: k-omega Shear Stress Transport (SST). [online]. 2019 [Accessed 2019-05-19]. Available from: <https://www.openfoam.com/documentation/guides/latest/doc/guide-turbulence-ras-k-omega-sst.html>
- [15] Andersson B., et. al.: Computational Fluid Dynamics for Engineers. Cambridge University Press, 2012

- [16] Ferziger J., Perić M.: Computational Methods for Fluid Dynamics. Springer-Verlag, 2002
- [17] ANSYS Fluent User's Guide, Release 15.0. ANSYS, Inc., 2013
- [18] Guerrero J.: Tips and tricks in OpenFOAM®. [online]. 2018 [Accessed 2019-05-19].  
Available from: <http://www.wolfdynamics.com/wiki/OFtipsandtricks.pdf>
- [19] Nguyen L., et. al.: Simulator Study of Stall/Post-Stall Characteristics of a Fighter Airplane With Relaxed Longitudinal Static Stability. National Aeronautics and Space Administration, TP-1538, 1979